LETTER

doi:10.1038/nature17398

The genetic program for cartilage development has deep homology within Bilateria

Oscar A. Tarazona[1,2], Leslie A. Slota[3], Davys H. Lopez[3], GuangJun Zhang[2]† & Martin J. Cohn[1,2,3]

The evolution of novel cell types led to the emergence of new tissues and organs during the diversification of animals[1]. The origin of the chondrocyte, the cell type that synthesizes cartilage matrix, was central to the evolution of the vertebrate endoskeleton. Cartilage-like tissues also exist outside the vertebrates, although their relationship to vertebrate cartilage is enigmatic. Here we show that protostome and deuterostome cartilage share structural and chemical properties, and that the mechanisms of cartilage development are extensively conserved—from induction of chondroprogenitor cells by Hedgehog and β-catenin signalling, to chondrocyte differentiation and matrix synthesis by SoxE and SoxD regulation of clade A fibrillar collagen (*ColA*) genes—suggesting that the chondrogenic gene regulatory network evolved in the common ancestor of Bilateria. These results reveal deep homology of the genetic program for cartilage development in Bilateria and suggest that activation of this ancient core chondrogenic network underlies the parallel evolution of cartilage tissues in Ecdysozoa, Lophotrochozoa and Deuterostomia.

Cartilage forms the embryonic endoskeleton of all vertebrates and has been widely considered to be a vertebrate-specific tissue[2,3]. This endoskeletal connective tissue is formed by non-adjacent cells embedded in abundant extracellular matrix (ECM) that is rich in collagen and acidic glycosaminoglycans (GAGs)[4,5]. Cartilage-like tissues have been recognized in invertebrate species scattered throughout the Protostomia (Fig. 1a); however, the relationship of these tissues to the bona fide cellular cartilage of vertebrates has long been debated[4,6,7] and the evolutionary origin of cartilage and its parent cell type, the chondrocyte, is unknown[4,8–10].

To determine whether invertebrate cartilage-like tissues have structural and/or chemical similarities to vertebrate cartilage, we compared the structure and matrix composition of these tissues in adults of two distantly related protostomes, the cuttlefish *Sepia bandensis* from the Lophotrochozoa and the horseshoe crab *Limulus polyphemus* from the Ecdysozoa, which are among the best known examples of invertebrate cartilage-like tissues[4,11]. Cartilage-like tissues in both species are composed of cells embedded in abundant ECM rich in collagen and acidic GAGs, and form conspicuous endoskeletal structures (Figs 1b–g and 2a–c, m, n and Supplementary Video 1). We then investigated chondrogenesis in *Sepia* and *Limulus*. In both species, cartilage development begins during late stages of organogenesis with the formation of pre-chondrogenic mesenchymal cell condensations that later secrete an ECM rich in collagen and acidic GAGs, mirroring the process of vertebrate chondrogenesis (Extended Data Fig. 1).

To test whether a common genetic program for cartilage development is conserved across the Bilateria, we asked whether *Sepia* and *Limulus* cartilages express pro-orthologues of the vertebrate collagen2α1 (*Col2α1*) gene, which encodes type II collagen, the most abundant protein in vertebrate cartilage ECM. We isolated two clade A collagen (*ColA*) genes from *Sepia* and one from *Limulus*

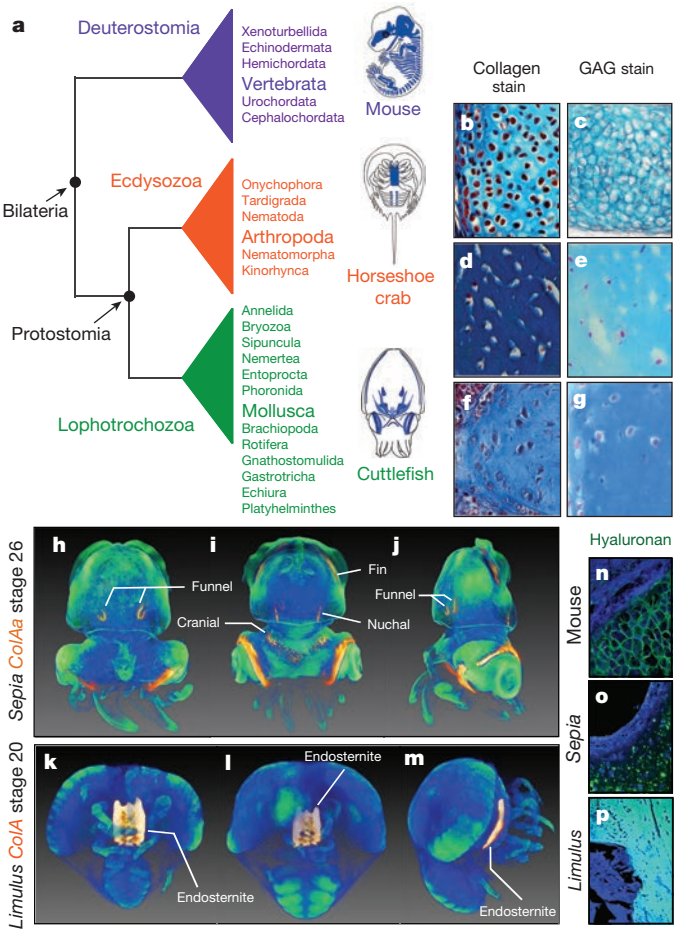

Figure 1 | Protostome invertebrate cartilage is structurally similar to vertebrate cartilage. a, Cartilage has evolved in Deuterostomia, Ecdysozoa and Lophotrochozoa. Cartilaginous endoskeletons of mouse, *Limulus* and *Sepia* are shown in blue (see also Supplementary Video 1). **b**–**g**, Sections through cartilage of mouse vertebra (**b**, **c**), horseshoe crab endosternite (**d**, **e**) and cuttlefish funnel (**f**, **g**). Masson's trichrome stain shows high content of collagen (**b**, **d**, **f**) and alcian blue stain shows high content of acidic GAGs (**c**, **e**, **g**) in all three cartilages. **h**–**m**, *ColA* expression in *Sepia* (**h**–**j**) and *Limulus* (**k**–**m**) embryos scanned with optical projection tomography (see Supplementary Videos 2 and 3). **h**–**j**, *ColAa* transcripts in *Sepia* embryos localize to numerous cartilages during chondrogenesis. **k**–**m**, *ColA* transcripts in the endosternite cartilage of *Limulus* embryos. Embryos shown in ventral (**h**, **k**), dorsal (**i**, **l**), and lateral (**j**, **m**) orientations. **n**–**p**, Cartilage ECM in vertebrates and protostomes is positive for hyaluronan.

[1]Howard Hughes Medical Institute, UF Genetics Institute, University of Florida, PO Box 103610, Gainesville, Florida 32610, USA. [2]Department of Biology, University of Florida, PO Box 103610, Gainesville, Florida 32610, USA. [3]Department of Molecular Genetics and Microbiology, University of Florida College of Medicine, PO Box 103610, Gainesville, Florida 32610, USA.
†Present address: Department of Comparative Pathobiology, Purdue University College of Veterinary Medicine, 625 Harrison Street, West Lafayette, Indiana 47907, USA.

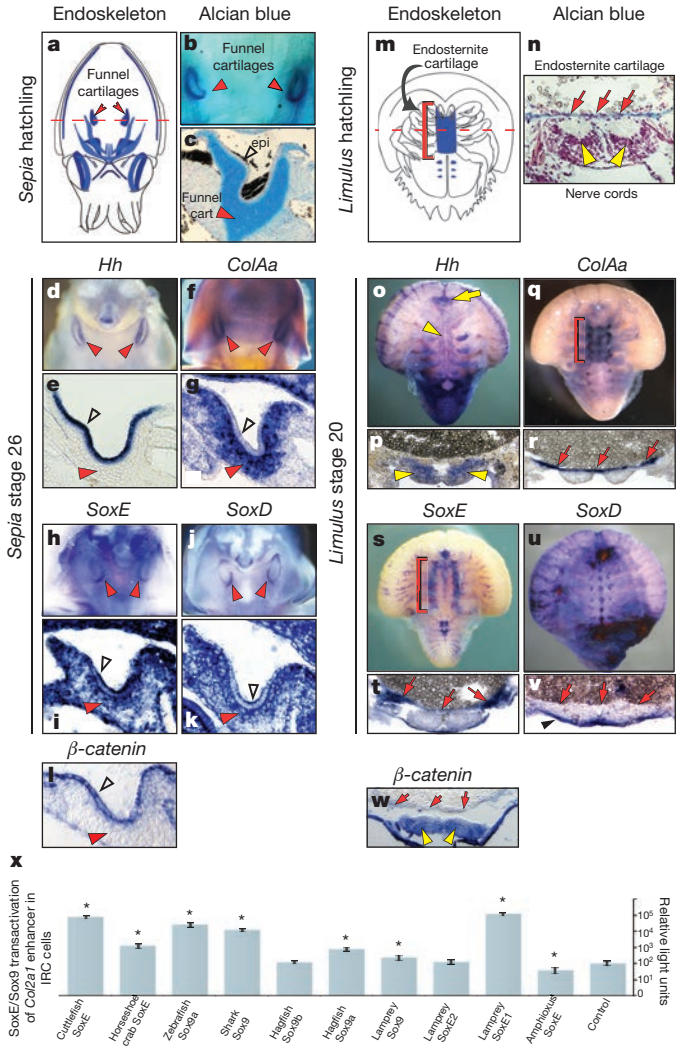

Figure 2 | Deep conservation of gene expression during protostome cartilage development. a, The *Sepia* hatchling endoskeleton. Dashed line indicates the plane of sections at the funnel cartilages (red arrowheads). **b**–**c**, Funnel cartilage in hatchlings stained with alcian blue in whole-mount (**b**) and in section (**c**). Cartilage, red arrowhead; funnel epithelium, black open arrowhead. **d**–**l**, Gene expression in *Sepia* embryos during chondrogenesis of funnel cartilage. Cartilage precursors in whole-mounts (**d**, **f**, **h** and **j**) and on sections (**e**, **g**, **i**, **k** and **l**), red arrowheads; funnel epithelium (**e**, **g**, **i**, **k** and **l**), open arrowheads. **m**, The *Limulus* hatchling endoskeleton. Dashed line indicates the plane of sections at the endosternite cartilage (red bracket). **n**, Endosternite cartilage (red arrows) of *Limulus* hatchling stained with alcian blue, located dorsal to the two nerve cords (yellow arrowheads). **o**–**w**, Gene expression during endosternite chondrogenesis in *Limulus* embryos. Nerve cords in whole-mounts (**o**) and on sections (**p**, **w**), yellow arrowheads; brain (**o**), yellow arrow. Pre-chondrogenic domains of endosternite chondrogenesis in whole-mounts (**o**, **q**, **s** and **u**), red brackets; and on sections (**p**, **r**, **t**, **v**, **w**), red arrows; ectoderm (**v**), black arrowhead. **x**, Luciferase reporter assay of SoxE/Sox9 transactivation of the human *COL2A1* enhancer in IRC cells. Significant differences over control (two-tailed *t*-test; $P < 0.05$; $n = 4$), asterisks; error bars, s.d. Each luciferase experiment was repeated four times, with four replicates per experiment.

(Extended Data Fig. 2) and analysed their expression during cartilage formation in both species. In *Sepia* embryos at stage 26, *ColAa* and *ColAb* expression localized to numerous regions of chondrogenesis, including the funnel, nuchal, fin and cranial cartilages (Fig. 1h–j, Extended Data Fig. 3 and Supplementary Video 2). Similarly, in *Limulus* embryos at stage 20, we detected *ColA* expression in the developing endosternite (Fig. 1k–m and Supplementary Video 3) and gill cartilages (Fig. 2q).

Hyaluronan, a non-sulfated GAG, is an essential component of vertebrate cartilage[12,13]. Although largely absent outside vertebrates, purification from a mollusc[14] led us to screen for hyaluronan in invertebrate cartilage. Using a hyaluronan binding peptide, we determined that *Sepia* and *Limulus* cartilage ECM is positive for hyaluronan (Fig. 1n–p). Hyaluronan synthases, however, could not be identified in protostome transcriptomic and genomic databases, suggesting that (1) hyaluronan could be synthesized by alternative mechanisms, (2) hyaluronan synthases could be present but unidentified in these groups or (3) hyaluronan synthases evolved multiple times, perhaps from chitin synthases, as proposed for the origin of vertebrate hyaluronan synthases[15]. The discovery of *ColA* and hyaluronan in these tissues reveals that key structural molecular components of cartilage are shared between invertebrate and vertebrate cartilages, and suggests that invertebrate cartilage is fibrillar-collagen-based.

We next investigated whether cell signalling proteins and transcription factors that function upstream of *Col2α1* in vertebrate chondrogenesis also are expressed during invertebrate chondrogenesis. The Hedgehog signalling pathway plays essential roles in early vertebrate chondrogenesis, where Shh regulates transcriptional activation of *Sox5/6/9* and Ihh regulates cartilage proliferation and differentiation[16–18]. We cloned *Hh* from *Sepia*, and analysis of its expression revealed that cartilage differentiation takes place in close proximity to *Hh* expression domains (Fig. 2d, e and Extended Data Fig. 4). In *Sepia* embryos at stage 26, *ColAa* and *ColAb* are expressed in a 'U-shaped' domain of mesenchymal pre-cartilaginous cells immediately adjacent to the *Hh*-expressing epithelium, in the region that will later form the funnel cartilage (Fig. 2d–g and Extended Data Fig. 4a, b).

Downstream of Hedgehog signalling, vertebrate Sox9, Sox5 and Sox6 function as master regulators of chondrogenesis by directly activating transcription of *Col2α1* (refs 19–21). We isolated invertebrate pro-orthologues of *Sox9* and *Sox5/Sox6*—*SoxE* and *SoxD*, respectively (Extended Data Fig. 2)—and found that *Sepia* funnel cartilage condensations express both *SoxE* (Fig. 2h, i and Extended Data Fig. 5) and *SoxD* (Fig. 2j, k and Extended Data Fig. 5), mirroring the demarcation of vertebrate cartilage condensations by *Sox9* and *Sox5/6* (ref. 20). Thus, as in vertebrates, *SoxE*, *SoxD* and *ColA* are co-expressed in the developing cartilaginous skeleton of *Sepia* embryos (Fig. 2f–k).

Sox9 and β-catenin have opposing functions in vertebrate chondrogenesis: they inhibit each other's transcriptional activity and β-catenin functions as an anti-chondrogenic transcriptional regulator[22–24]. Indeed, reduction of *β-catenin* mRNA and protein levels in *Sox9*-positive chondroprogenitor cells is necessary for cartilage differentiation[22–24]. To test whether this regulatory relationship is conserved in *Sepia* cartilage, we cloned *β-catenin* and found that it is expressed in funnel mesenchyme and in the overlying epithelium at stages 24–25 (Extended Data Fig. 5e), but by stage 26, *β-catenin* mRNA is undetectable in pre-cartilaginous condensations (Fig. 2l). As in vertebrates, downregulation of *β-catenin* in *Sepia* chondroprogenitors precedes the onset of differentiation (Extended Data Fig. 1).

To test whether conservation of a core chondrogenic network extends to Ecdysozoa, we cloned and analysed expression of *Hh*, *SoxE*, *SoxD* and *β-catenin* during *Limulus* chondrogenesis. In *Limulus* embryos, the endosternite cartilage forms immediately adjacent to the *Hh*-expressing ventral nerve cords (Fig. 2o–p and Extended Data Fig. 1). The pre-chondrogenic condensation of the endosternite can be identified as a thin plate of *ColA*-expressing cells dorsal to the paired nerve cords (Fig. 2q, r). Similarly, *SoxE* is expressed throughout the developing endosternite plate (Fig. 2s, t) and gill cartilages (Extended Data Fig. 6c), although *SoxD* was not detectable in these tissues (Fig. 2u–v). In *Limulus*, as in *Sepia* and vertebrates, *β-catenin* is downregulated in *SoxE*/*ColA*-expressing cells before cartilage differentiation (Fig. 2w). Taken together, our analysis of *Sepia* and *Limulus* chondrogenesis indicates that the network of structural and regulatory genes required for vertebrate cartilage development has deeply conserved patterns of expression in the three major lineages of Bilateria.

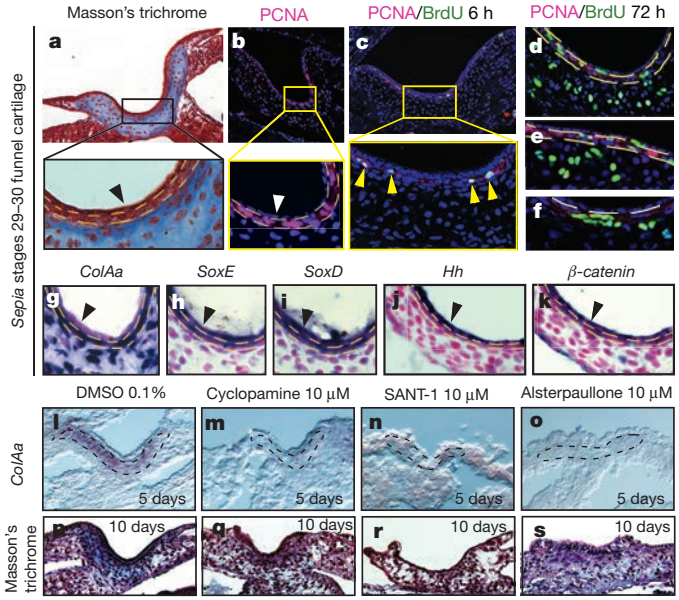

Figure 3 | Cuttlefish chondrogenesis is regulated positively by *Hh* signalling and negatively by *β-catenin*. **a**, At stages 29–30 a non-cartilaginous, undifferentiated cell layer (yellow broken line outline) lies below the funnel epithelium (black arrowhead). **b**, Proliferating cell nuclear antigen (PCNA) immunoreactivity indicates cell proliferation is restricted to this undifferentiated cell layer (between yellow broken lines); funnel epithelium, white arrowhead. **c**–**f**, Pulse-chase assay of BrdU incorporation at (**c**) 6 h exposure and (**d**–**f**) 72 h of incubation after initial exposure. At 6 h, PCNA/BrdU are co-localized to the proliferative zone (yellow arrowheads). After 72 h, labelled cells advance into the funnel cartilage (**d**–**e**) and also contribute to the cell pool in the proliferative zone (**f**). Broken white line marks basal lamina of funnel epithelium. **g**–**k**, The proliferative zone expresses *ColAa* (**g**), *SoxE* (**h**), *SoxD* (**i**), and *β-catenin* (**k**); the funnel epithelium expresses *Hh* (**j**) and *β-catenin* (**k**). **l**–**o**, *ColAa* expression in the funnel region after 5 days of treatment with cyclopamine, SANT-1 and alsterpaullone ($n = 4$ embryos each treatment). In DMSO controls, pre-cartilaginous mesenchyme (outlined by dashed lines) expresses *ColAa* (**l**), whereas *ColAa* is undetectable in the funnel of embryos treated with (**m**) cyclopamine, (**n**) SANT-1 or (**o**) alsterpaullone. **p**–**s**, Masson's trichrome staining of funnel region after 10 days of treatment ($n = 4$ embryos per treatment) shows that DMSO control embryos undergo cartilage differentiation (**t**), but embryos treated with cyclopamine (**q**), SANT-1 (**r**) or alsterpaullone (**s**) do not differentiate into cartilage and lack a collagenous matrix (see Supplementary Table 4 for number of embryos treated and analysed).

To determine whether invertebrate SoxE proteins could function as transcriptional regulators of *ColA* genes, we tested the ability of *Sepia* and *Limulus* SoxE proteins to activate the human *COL2A1* cartilage-specific enhancer[25] using a luciferase reporter assay in NIH3T3 and immortalized rat chondrocyte (IRC) cells. Quantification of luciferase activity revealed significant transactivation by *Sepia* and *Limulus* SoxE, with efficiencies equal to or greater than Sox9/SoxE from lamprey, hagfish, shark and zebrafish (Fig. 2x and Extended Data Fig. 5). Thus, *Sepia* and *Limulus* SoxE proteins have transactivation functions similar to vertebrate Sox9 proteins.

Vertebrate cartilage growth occurs by progression of chondrocytes from resting zones (at the epiphyseal ends) into the zones of proliferation, maturation and hypertrophy[26]. Prehypertrophic cells secrete Ihh, which regulates proliferation and differentiation of adjacent chondrocytes[26]. In *Sepia* embryos at stages 29–30, we observed an undifferentiated layer of proliferating cells between the *Hh*-expressing funnel epithelium and the overtly differentiated chondrocytes (Fig. 3a, b). To test whether *Sepia* funnel cartilage growth involves directional proliferation and maturation, similar to vertebrate cartilage, we performed a pulse-chase 5-bromo-2′-deoxyuridine (BrdU) assay. Chondroprogenitor cells labelled in the proliferative zone (Fig. 3c) were later found deep in the funnel cartilage (Fig. 3d–f), indicating directional growth. Restriction of proliferating cells to the perimeter of the funnel cartilage, adjacent to *Hh*-expressing cells, and expression of *SoxE*, *SoxD*, *β-catenin* and *ColAa*/*ColAb* in this highly-proliferative undifferentiated layer suggest that appositional growth of the *Sepia* funnel cartilage occurs at the ends of the element, reminiscent of the growth pattern of vertebrate cartilage (Fig. 4a).

We then tested whether expression of *Hh* and degradation of β-catenin are necessary for *ColA* expression and differentiation of funnel cartilage in *Sepia*, as is the case in vertebrates[22–26]. We used the small molecules cyclopamine and SANT-1 (inhibitors of Smoothened) to block Hh signalling[27] and alsterpaullone (inhibitor of GSK-3β) to stabilize β-catenin[28]. Five-day treatments were initiated at stages 23–24, before formation of pre-cartilaginous cell condensations but after the appearance of the funnel epithelium and associated mesenchyme. Hh antagonism or β-catenin stabilization resulted in loss of *ColAa* expression in funnel chondroprogenitor cells by stage 26 (Fig. 3l–o). Although *ColA* expression was not maintained, funnel chondroprogenitors continued to proliferate and express *β-catenin* and funnel epithelium continued to express *Hh* (Extended Data Figs 7, 8 and 9n, o), indicating that loss of *ColAa* was not due to toxicity or global effects on transcription.

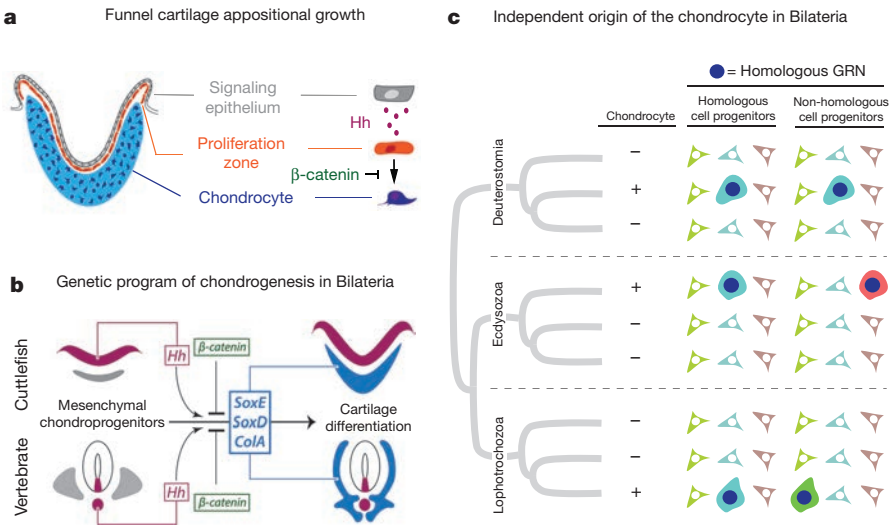

Figure 4 | Bilaterian cartilage development and the origin of the chondrocyte. **a**, Model of cuttlefish funnel cartilage appositional growth. New cartilage is derived from a proliferative layer of chondrocyte precursors. **b**, Conservation of the developmental genetic program of cartilage development between vertebrates and invertebrates. Vertebrate cartilage represented by a mouse vertebra and invertebrate cartilage by a *Sepia* funnel cartilage. **c**, Two hypotheses for independent evolution of cartilage are presented. The homologous cell progenitors model depicts the independent origin of the chondrocyte through the recruitment of a homologous gene regulatory network (GRN; dark blue circle) by the same homologous progenitor cell type (blue fibroblasts) across Bilateria. Alternatively, the non-homologous cell progenitors model depicts independent evolution by activation of the same homologous gene regulatory network but in different, non-homologous progenitor cell types (blue, red and green fibroblasts). See Supplementary Discussion for further details.

Prolonged inhibition of *ColA* in *Sepia* prevented differentiation of cartilage tissue. When embryos were cultured for 10 days, to stage 28, in the presence of Smo antagonists (cyclopamine or SANT-1) or GSK-3β inhibitors (alsterpaullone or BIO), funnel cartilage differentiation was inhibited (Fig. 3q–s and Extended Data Fig. 9a). By contrast, embryos treated with dimethylsulfoxide (DMSO) alone (controls) or with the β-catenin signalling repressors IWR-1 or PNU underwent normal funnel cartilage differentiation, including generation of a conspicuous cartilage ECM (Fig. 3p and Extended Data Fig. 9b, c). Taken together, our finding that Hh and β-catenin signalling have opposite effects on chondrogenesis both in cuttlefish and in vertebrates demonstrates deep conservation of the genetic program for chondrogenesis in Bilateria (Fig. 4b)

Although a single origin of the bilaterian chondrocyte is still plausible, we posit two hypotheses that can account for independent origins of the chondrocyte (Fig. 4c and Supplementary Discussion). In the first scenario, the chondrocyte evolved in parallel, but from a homologous fibroblast-like cell type, in different lineages of Bilateria by recruitment of a homologous gene regulatory network (Fig. 4c). One possible chondroid precursor cell that could have been recruited in parallel in Bilateria is the mesodermal midline cell type that gives rise to the deuterostome notochord and the protostome axochord[29]. However, a variety of cell/tissue types in invertebrate deuterostomes activate components of the chondrogenic gene regulatory network during histogenesis of non-cartilaginous endoskeletal tissues[10,30]. Therefore, an alternative hypothesis is that chondrocytes evolved in parallel by activation of the same gene regulatory network but in non-homologous cell types across the Bilateria (Fig. 4c). Taken together, our data suggest that the core kernel of the chondrogenic gene network that orchestrates cartilage development was probably present in the urbilaterian ancestor and may have been involved in the production of a specialized ECM type. Finally, our results raise the potential for the emergence of invertebrates as new model systems for the study of chondrogenesis, cartilage physiology and regeneration.

Online Content Methods, along with any additional Extended Data display items and Source Data, are available in the online version of the paper; references unique to these sections appear only in the online paper.

Received 18 July 2014; accepted 4 February 2016.
Published online 25 April 2016.

1. Arendt, D. The evolution of cell types in animals: emerging principles from molecular studies. *Nature Rev. Genet.* **9,** 868–882 (2008).
2. Gans, C. & Northcutt, R. G. Neural crest and the origin of vertebrates: a new head. *Science* **220,** 268–273 (1983).
3. Meulemans, D. & Bronner-Fraser, M. Insights from amphioxus into the evolution of vertebrate cartilage. *PLoS ONE* **2,** e787 (2007).
4. Person, P. & Philpott, D. E. The nature and significance of invertebrate cartilages. *Biol. Rev. Camb. Phil. Soc.* **44,** 1–16 (1969).
5. Zhang, G., Eames, B. F. & Cohn, M. J. Chapter 2. Evolution of vertebrate cartilage development. *Curr. Top. Dev. Biol.* **86,** 15–42 (2009).
6. Schaffer, J. in *Handbuch der mikroskopischen Anatomie des Menschen* Vol. 2 (2) (ed. W von Möllendorf) 1–390 (Springer, 1930).
7. Cowden, R. R. A histochemical study of chondroid tissue in *Limulus* and *Octopus*. *Histochemie* **9,** 149–163 (1967).
8. Hall, B. K. & Gillis, J. A. Incremental evolution of the neural crest, neural crest cells and neural crest-derived skeletal tissues. *J. Anat.* **222,** 19–31 (2013).
9. Cole, A. G. & Hall, B. K. Cartilage is a metazoan tissue; integrating data from nonvertebrate sources. *Acta Zool.* **85,** 69–80 (2004).
10. Zhang, G. & Cohn, M. J. Hagfish and lancelet fibrillar collagens reveal that type II collagen-based cartilage evolved in stem vertebrates. *Proc. Natl Acad. Sci. USA* **103,** 16829–16833 (2006).
11. Cole, A. G. & Hall, B. K. The nature and significance of invertebrate cartilages revisited: distribution and histology of cartilage and cartilage-like tissues within the Metazoa. *Zoology* **107,** 261–273 (2004).
12. Roughley, P. J. The structure and function of cartilage proteoglycans. *Eur. Cell. Mater.* **12,** 92–101 (2006).
13. Matsumoto, K. *et al.* Conditional inactivation of Has2 reveals a crucial role for hyaluronan in skeletal growth, patterning, chondrocyte maturation and joint formation in the developing limb. *Development* **136,** 2825–2835 (2009).
14. Volpi, N. & Maccari, F. Purification and characterization of hyaluronic acid from the mollusc bivalve *Mytilus galloprovincialis*. *Biochimie* **85,** 619–625 (2003).
15. DeAngelis, P. L. Evolution of glycosaminoglycans and their glycosyltransferases: implications for the extracellular matrices of animals and the capsules of pathogenic bacteria. *Anat. Rec.* **268,** 317–326 (2002).
16. Zeng, L., Kempf, H., Murtaugh, L. C., Sato, M. E. & Lassar, A. B. Shh establishes an Nkx3.2/Sox9 autoregulatory loop that is maintained by BMP signals to induce somitic chondrogenesis. *Genes Dev.* **16,** 1990–2005 (2002).
17. Abzhanov, A. & Tabin, C. J. Shh and Fgf8 act synergistically to drive cartilage outgrowth during cranial development. *Dev. Biol.* **273,** 134–148 (2004).
18. Kronenberg, H. M. Developmental regulation of the growth plate. *Nature* **423,** 332–336 (2003).
19. Akiyama, H., Chaboissier, M. C., Martin, J. F., Schedl, A. & de Crombrugghe, B. The transcription factor Sox9 has essential roles in successive steps of the chondrocyte differentiation pathway and is required for expression of Sox5 and Sox6. *Genes Dev.* **16,** 2813–2828 (2002).
20. Smits, P. *et al.* The transcription factors L-Sox5 and Sox6 are essential for cartilage formation. *Dev. Cell* **1,** 277–290 (2001).
21. Lefebvre, V., Li, P. & de Crombrugghe, B. A new long form of Sox5 (L-Sox5), Sox6 and Sox9 are coexpressed in chondrogenesis and cooperatively activate the type II collagen gene. *EMBO J.* **17,** 5718–5733 (1998).
22. Hill, T. P., Später, D., Taketo, M. M., Birchmeier, W. & Hartmann, C. Canonical Wnt/β-catenin signaling prevents osteoblasts from differentiating into chondrocytes. *Dev. Cell* **8,** 727–738 (2005).
23. Day, T. F., Guo, X., Garrett-Beal, L. & Yang, Y. Wnt/β-catenin signaling in mesenchymal progenitors controls osteoblast and chondrocyte differentiation during vertebrate skeletogenesis. *Dev. Cell* **8,** 739–750 (2005).
24. Akiyama, H. *et al.* Interactions between Sox9 and β-catenin control chondrocyte differentiation. *Genes Dev.* **18,** 1072–1087 (2004).
25. Lefebvre, V. *et al.* A 47-bp sequence of the first intron of the mouse proα1(II) collagen gene is sufficient to direct chondrocyte expression. *Ann. NY Acad. Sci.* **785,** 284–287 (1996).
26. St-Jacques, B., Hammerschmidt, M. & McMahon, A. P. Indian hedgehog signaling regulates proliferation and differentiation of chondrocytes and is essential for bone formation. *Genes Dev.* **13,** 2072–2086 (1999).
27. Grimaldi, A. *et al.* A hedgehog homolog is involved in muscle formation and organization of *Sepia officinalis* (Mollusca) mantle. *Dev. Dynam.* **237,** 659–671 (2008).
28. Broun, M., Gee, L., Reinhardt, B. & Bode, H. R. Formation of the head organizer in hydra involves the canonical Wnt pathway. *Development* **132,** 2907–2916 (2005).
29. Lauri, A. *et al.* Development of the annelid axochord: insights into notochord evolution. *Science* **345,** 1365–1368 (2014).
30. Rychel, A. L. & Swalla, B. J. Development and evolution of chordate cartilage. *J. Exp. Zool. B* **308,** 325–335 (2007).

Supplementary Information is available in the online version of the paper.

Author Contributions O.A.T. and M.J.C. designed the experiments, analysed the data and wrote the paper. O.A.T., L.A.S. and D.H.L. cloned *Sepia* and *Limulus* genes, analysed gene and protein expression, and performed histological analysis of adult tissues. O.A.T. isolated the full-length *ColA* cDNA, performed the optical projection tomography scanning and three-dimensional reconstructions, BrdU and small-molecule treatments, and the experiments on treated and control embryos. G.Z. isolated the full-length *Sox9/SoxE* genes and prepared the expression constructs for amphioxus, lamprey, hagfish and shark, and O.A.T. for zebrafish, cuttlefish and horseshoe crab. O.A.T. performed the cell culture and luciferase assays.

Acknowledgements We thank B. Battelle and members of H. J. Brockmann's and David Julian's laboratories for *Limulus* eggs, N. Brown for sharing protocols and reagents, N. Patel and the *Limulus* genome consortium for access to sequence data, and M. Welten and F. Leal for assisting with optical projection tomography and luciferase assays, respectively. This project was supported by the Howard Hughes Medical Institute (to M.J.C.). O.A.T. was a Howard Hughes Medical Institute International Student Research Fellow.

Author Information Sequences generated in this work have been deposited in GenBank under accession numbers KP322116–KP322126. Reprints and permissions information is available at www.nature.com/reprints. The authors declare no competing financial interests. Readers are welcome to comment on the online version of the paper. Correspondence and requests for materials should be addressed to M.J.C. (mjcohn@ufl.edu).

METHODS

No statistical methods were used to predetermine sample size. Embryos were randomized in each experiment. The investigators were not blinded to allocation during experiments and outcome assessment.

Embryo collection and preparation. *Sepia phraonis* eggs were obtained from the National Resource Center for Cephalopods, Galveston, Texas, USA. *S. bandensis* and *Sepia officinalis* eggs were purchased from commercial suppliers. Upon arrival at our institution, eggs were cultured in artificial seawater (Petco Real Ocean Water) at 22 °C. Embryos were collected by manual removal of egg cases and were staged according to ref. 31. Embryos used for *in situ* hybridization (ISH) and immunohistochemistry were fixed and processed as previously described[27]. *Limulus* embryos were provided by B. Battelle and members of H. J. Brockmann's and D. Julian's laboratories and were staged according to ref. 32 and processed for ISH as previously described[33].

Alcian blue and Masson's trichrome stain. Cartilage was stained with alcian blue staining to reveal GAGs. In vertebrate cartilage, alcian blue can detect highly anionic GAGs, such as hyaluronan and sulfated GAGs. Early biochemical analyses of cartilaginous tissues in cephalopods and horseshoe crabs suggested the presence of highly sulfated GAGs, such as chondroitin sulfate[34–36]. To detect GAGs in *Sepia* and *Limulus* cartilage, we used alcian blue/nuclear fast red staining on paraffin sections. Deparaffinized sections were stained for 30 min in 1% alcian blue (in 3% acetic acid) and counter stained with nuclear fast red for 5 min. Masson's trichrome staining was performed on paraffin sections using a Masson's Trichrome Kit (22-110-648, Richard-Allan Scientific) following the manufacturer's instructions.

Gene cloning and rapid amplification of cDNA ends PCR (RACE–PCR). RNA extraction from *Sepia* embryos at stages 24–26 and from *Limulus* stages 19–20 was done using TRIzol reagent (Ambion) following the manufacturer's instructions. cDNA synthesis was performed by an AMV reverse transcriptase (New England Biolabs) following the manufacturer's instructions. PCR amplification was carried using the following primers SepiaSoxEr, TGCTACCATGTTAGAAGTCATGCCT; SepiaSoxEf, GATTACCCTGATTACAAATACCAGCCC; SepiaSoxDf, CCACTACCAGCTCATAGCAACCATCAG; SepiaSoxDr, GGGCTTTGAGG GGTCAGGTTTCTCT; SepiaColAaf, AACGCCCCTGCCCGTTCCTGTCGC GATC; SepiaColAar, TCCCAATTCTATATGGAAGTCTTGT; Sepiahhf, TAATG TATCGGAAAACACAGTTGGTGCCA; Sepiahhr, GAGGAAGGCGATGA CTTCGCTGTAA; SepiabetacateninF1, TGTGCTGCTGGCATTCTGTCCAATC; SepiabetacateninR1, GCGACTCCTTCGTTCCTGGAGTGTA; LimulusSoxDF, CCAAAGAGAACTTGTATTGTGGATGGC; LimulusSoxDR, GGTGTCTG TCTCTCAGCTTGAAACATACCA; LimulusSoxEF, TTGCATGGACAA ACTCGTCAACTCGGT; LimulusSoxER, GGAAACTGGATACTGATGATAT GGAGTATC; LimulusColAaF, ATATGATGCAAGTGCTCTTGCTGCTCTCCT; LimulusColAaR, CTCACTGAAGAGTTGTAGGAAACTAAGCTG; LimulusHhF, GTCTTTAAGCARCAYGTNCCNAA; LimulusHhR, AAAGTTTGCGTACCART GDATNCC; LimulusbcatF, TTATGCCATCACTACCTTGCACAATCTC; LimulusbcatR, CTTGACAAGTGCAGGAATTCCCCCAGAT.

Full-length cDNA clones were isolated by rapid amplification of cDNA ends using SMARTer RACE 5′/3′ Kit (Clontech) and synthesis of 5′ and 3′ RACE cDNA libraries was performed following the manufacturer's instructions. The primers used in RACE–PCR experiments were as follows: HSCraceColAbr, GTAAAACGACGGCCA GTCGGCAGTGGTAGGTAATATTCTGTACAGC; SepPhRACEcolAbr, GTAAAACGACGGCCAGTCGGCAGTGGTAGGTAATATTCTGTACAGC; SepPhRACEcolAar, GTAAAACGACGGCCAGTGAGACAACCACACATAGGACTC TCCGGCT.

Sequences for *Sepia ColAa*, *ColAb*, *SoxE*, *SoxD*, *Hh* and *β-catenin*, and for *Limulus ColA*, *SoxE*, *SoxD*, *Hh* and *β-catenin*, have been deposited in GenBank under accession numbers KP322116–KP322126.

ISH and immunohistochemistry. Whole-mount ISH was performed using digoxigenin- and fluorescein-labelled antisense (or sense control) RNA probes according to protocols previously described for *Sepia*[27] and *Limulus*[33]. ISH on cryosections was performed using previously described protocols for vertebrate tissues[37]. PCNA, β-catenin and hyaluronan detection was performed on cryosections using mouse anti-PCNA (ab29, abcam), anti-β-catenin (C2206, Sigma-Aldrich) and biotinylated hyaluronic acid binding protein (385911, EMD Millipore). Hyaluronan detection on mouse, *Sepia* and *Limulus* cartilages was performed using streptavidin-HRP with Alexa Fluor 488 tyramide signal amplification (Molecular Probes).

ISH and phalloidin staining. Phalloidin staining was performed on cryosectioned embryos after whole-mount ISH. RNA expression was imaged by detecting the fluorescence generated by the NBT/BCIP precipitate emission (over 700 nm) when excited at 633 nm. Phalloidin staining was done using Alexa Fluor 488 phalloidin (Life Technologies). Sections were blocked with 1% BSA (A9647, Sigma-Aldrich) in PBS before a 30 min incubation with Alexa Fluor 488 phalloidin at 6.6 μM in blocking solution (1% BSA in PBS).

Optical projection tomography of embryos after ISH. *Sepia* and *Limulus* embryos were fixed in 4% paraformaldehyde in PBS after the completion of whole-mount ISH, and embryos were prepared and scanned following previously described protocols for vertebrate embryos[38,39]. Optical projection tomography scanning was performed using a Bioptonics 3001 OPT Scanner. The anatomy and gene expression channels were reconstructed using NRecon software and imported into the Amira program for three-dimensional visualization, analysis and renderings of three-dimensional images and videos.

Molecular phylogenetic analysis of *collagen* and *Sox* genes. Phylogenetic analyses of *collagen* and *Sox* sequences cloned from *Sepia* and *Limulus* cDNA pools were aligned with putative orthologues derived from EST databases (NCBI) by tBlastn searches using mouse *Col2a1* (AAH51383) and *Haliotis* collagen pro-alpha chain (BAA75668) collagens, and mouse *Sox9* (NP_035578) and *Sox6* (AAC52263). The retrieved sequences used for the phylogenetic analyses can be found in Supplementary Tables 1 and 2. Amino-acid sequences were aligned using MUSCLE[40] and phylogenetic reconstruction was performed with MrBayes 3.2.2 (ref. 41) using the WAG model[42] of amino-acid substitution, as described previously[43].

Treatments with small-molecule inhibitors. *S. officinalis* embryos were staged inside their egg cases after removing the outer layers of the egg case until the remaining inner layers were translucent enough to see the embryo. Embryos were selected for treatments once they reached stages 23–24, when they have already developed the funnel epithelium and associated mesenchyme (Extended Data Figs 7 and 8). Treatments were done in 100 ml glass beakers with 50 ml of sterile artificial seawater. Control embryos were treated with DMSO at 0.1%, and experimental embryos were exposed to 10 μM of cyclopamine (C988400, Toronto Research Chemicals), SANT-1 (S4572, Sigma-Aldrich), alsterpaullone (A4847, Sigma-Aldrich), BIO (B1686, Sigma-Aldrich), IWR-1 (I0161, Sigma), or PNU-74654 (P0052, Sigma-Aldrich) by adding 50 μl of 10 mM stock solutions for each of the drugs. DMSO was used as the solvent for all stock solutions. The following small-molecule inhibitors were used to target Hh and β-catenin signalling: cyclopamine and SANT-1 function as Smoothened inhibitors and antagonize Hh signalling; alsterpaullone and BIO function as agonists of β-catenin signalling by inhibiting GSK-3β (alsterpaullone has a broader spectrum and also inhibits other kinases, such as CDK1 and CDK5); IWR-1 and PNU-74654 work as antagonists of β-catenin signalling by inducing axin stabilization (stabilization of *β-catenin* destruction complex) and by blocking the interaction of β-catenin with Tcf, respectively.

Embryos were incubated in 22 °C seawater with the treatment drug or with DMSO. Seawater containing the drug at the appropriate final concentration (or DMSO for controls) was replaced every 2 days, for a total exposure period of either 5 days or 10 days. Specimens were then collected and fixed for histology or ISH, as described above.

BrdU labelling and BrdU pulse chase. *S. officinalis* eggs ($n = 8$) were incubated in 0.05% BrdU in seawater at 22 °C for 6 h. Four embryos were processed immediately for immunofluorescence after BrdU incubation; the rest of the eggs were rinsed several times in seawater free of BrdU, then washed five times every 10 min, then five times every 30 min, and finally incubated for 3 days with complete water changes every 24 h. Embryos were fixed overnight in 4% paraformaldehyde. BrdU labelling was detected with an anti-BrdU antibody (G3G4, DSHB) and immunofluorescence on cryosections. Antigen retrieval was performed with incubation for 30 min in 2 N HCl.

Luciferase assay. We used a firefly luciferase reporter construct controlled by the *Col2a1* promoter and the *Col2a1* chondrocyte-specific enhancer[44] (Extended Data Fig. 5f). We cloned full-length *SoxE* and *Sox9* from cDNA by reverse transcription PCR and ligated each into a pcDNA3.3 expression vector under the control of a CMV promoter (Invitrogen). Two cell lines, NIH3T3 mouse fibroblast (ATCC, CRL-1658) and IRC cells (a gift from W. Horton), were transfected using Lipofectamine 3000 (Invitrogen) with 200 ng of DNA per well (48-well plates) corresponding to the luciferase plasmid and the corresponding expression vector at a ratio of 1:3. We used the firefly luciferase vector and a Renilla luciferase control vector at a ratio of 20:1. After transfection, cells were cultured for 48 h as previously described[44] and luciferase activity was measured using a Dual-Luciferase Reporter Assay System (E1910, Promega) according to the manufacturer's instructions.

31. Lemaire, J. Table de developpement embryonnaire de *Sepia officinalis*. L. (mollusque cephalopode). *Bull. Soc. Zool. Fr.* **95,** 773–782 (1970).
32. Sekiguchi, K., Yamamichi, Y. & Costlow, J. D. Horseshoe crab developmental studies I. Normal embryonic development of *Limulus polyphemus* compared with *Tachypleus tridentatus*. *Prog. Clin. Biol. Res.* **81,** 53–73 (1982).
33. Blackburn, D. C. *et al.* Isolation and expression of Pax6 and atonal homologues in the American horseshoe crab, *Limulus polyphemus*. *Dev. Dynam.* **237,** 2209–2219 (2008).
34. Hall, B. K. *Bones and Cartilage: Developmental and Evolutionary Skeletal Biology* Ch. 4, 51–63 (Elsevier, 2005).

35. Sugahara, K. *et al.* Novel sulfated oligosaccharides containing 3-*O*-sulfated glucuronic acid from king crab cartilage chondroitin sulfate K. Unexpected degradation by chondroitinase ABC. *J. Biol. Chem.* **271,** 26745–26754 (1996).
36. Kinoshita, A. *et al.* Novel tetrasaccharides isolated from squid cartilage chondroitin sulfate E contain unusual sulfated disaccharide units GlcA(3-*O*-sulfate)β1–3GalNAc(6-*O*-sulfate) or GlcA(3-*O*-sulfate)β1–3GalNAc. *J. Biol. Chem.* **272,** 19656–19665 (1997).
37. Abzhanov, A. Darwin's finches: analysis of beak morphological changes during evolution. *Cold Spring Harbor Protoc.* **2009,** emo119 (2009).
38. Quintana, L. & Sharpe, J. Preparation of mouse embryos for optical projection tomography imaging. *Cold Spring Harb. Protoc.* **2011,** 664–669 (2011).
39. Quintana, L. & Sharpe, J. Optical projection tomography of vertebrate embryo development. *Cold Spring Harb. Protoc.* **2011,** 586–594 (2011).
40. Edgar, R. C. MUSCLE: multiple sequence alignment with high accuracy and high throughput. *Nucleic Acids Res.* **32,** 1792–1797 (2004).
41. Huelsenbeck, J. P. & Ronquist, F. MRBAYES: Bayesian inference of phylogenetic trees. *Bioinformatics* **17,** 754–755 (2001).
42. Whelan, S. & Goldman, N. A general empirical model of protein evolution derived from multiple protein families using a maximum-likelihood approach. *Mol. Biol. Evol.* **18,** 691–699 (2001).
43. Zhang, G., Miyamoto, M. M. & Cohn, M. J. Lamprey type II collagen and Sox9 reveal an ancient origin of the vertebrate collagenous skeleton. *Proc. Natl Acad. Sci. USA* **103,** 3180–3185 (2006).
44. Lefebvre, V., Huang, W., Harley, V. R., Goodfellow, P. N. & de Crombrugghe, B. SOX9 is a potent activator of the chondrocyte-specific enhancer of the pro alpha1(II) collagen gene. *Mol. Cell. Biol.* **17,** 2336–2346 (1997).

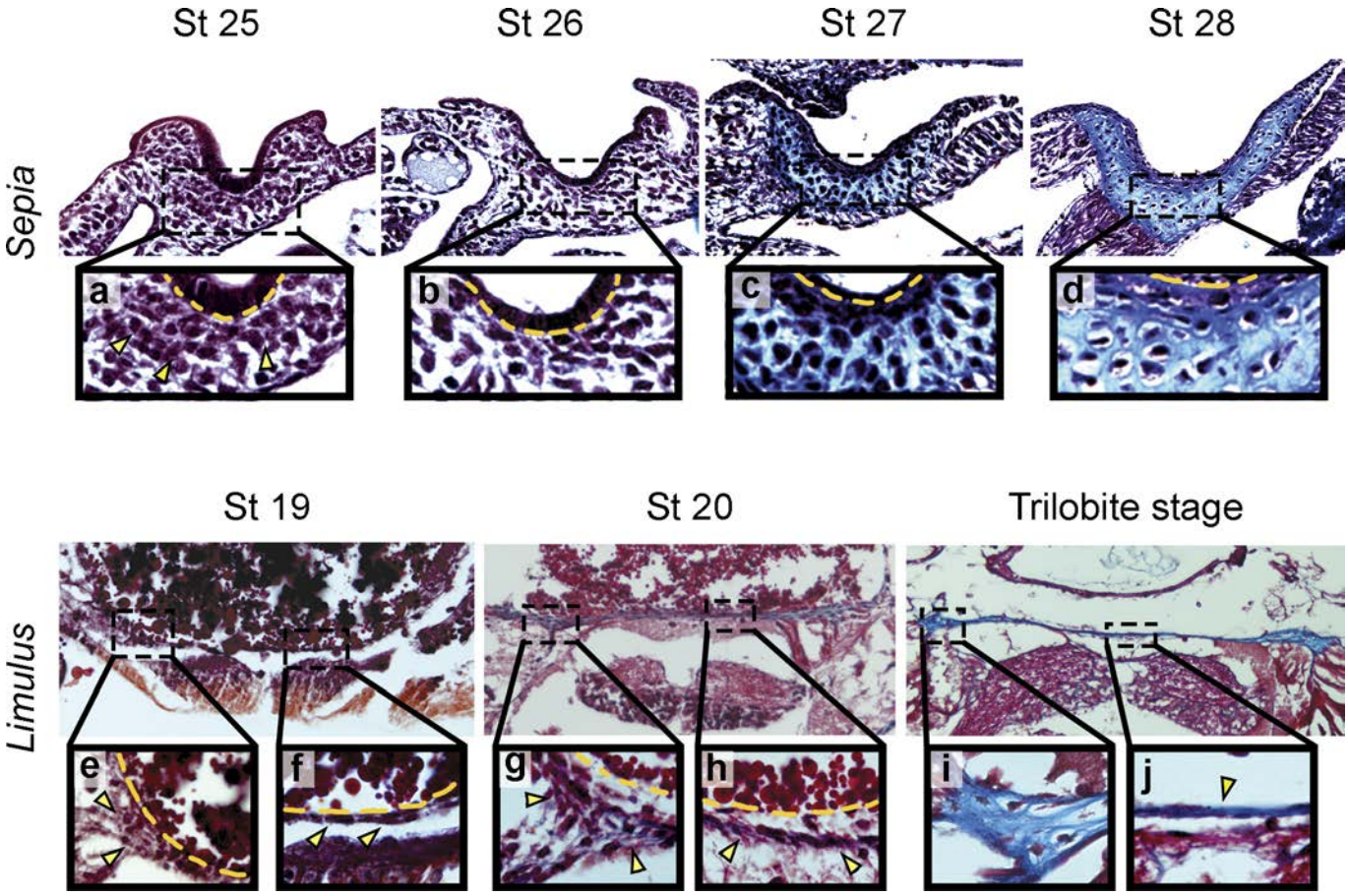

Extended Data Figure 1 | Developmental series showing chondrogenesis in *Sepia* and *Limulus*. Masson's trichrome-stained sections. Collagen is stained blue. **a**–**d**, Sections through funnel cartilage of *Sepia* embryos. Bottom row shows high magnification of boxed area. Yellow arrowheads mark the pre-cartilaginous cell condensation and the yellow dashed line marks the level of the basal lamina of the funnel epithelium. **e**–**j**, Transverse sections through the endosternite of *Limulus* embryos. Bottom row shows high magnification of boxed area. Yellow arrowheads mark the pre-cartilaginous cell condensations and the yellow dashed line delineates the mesenchyme from the yolk cavity.

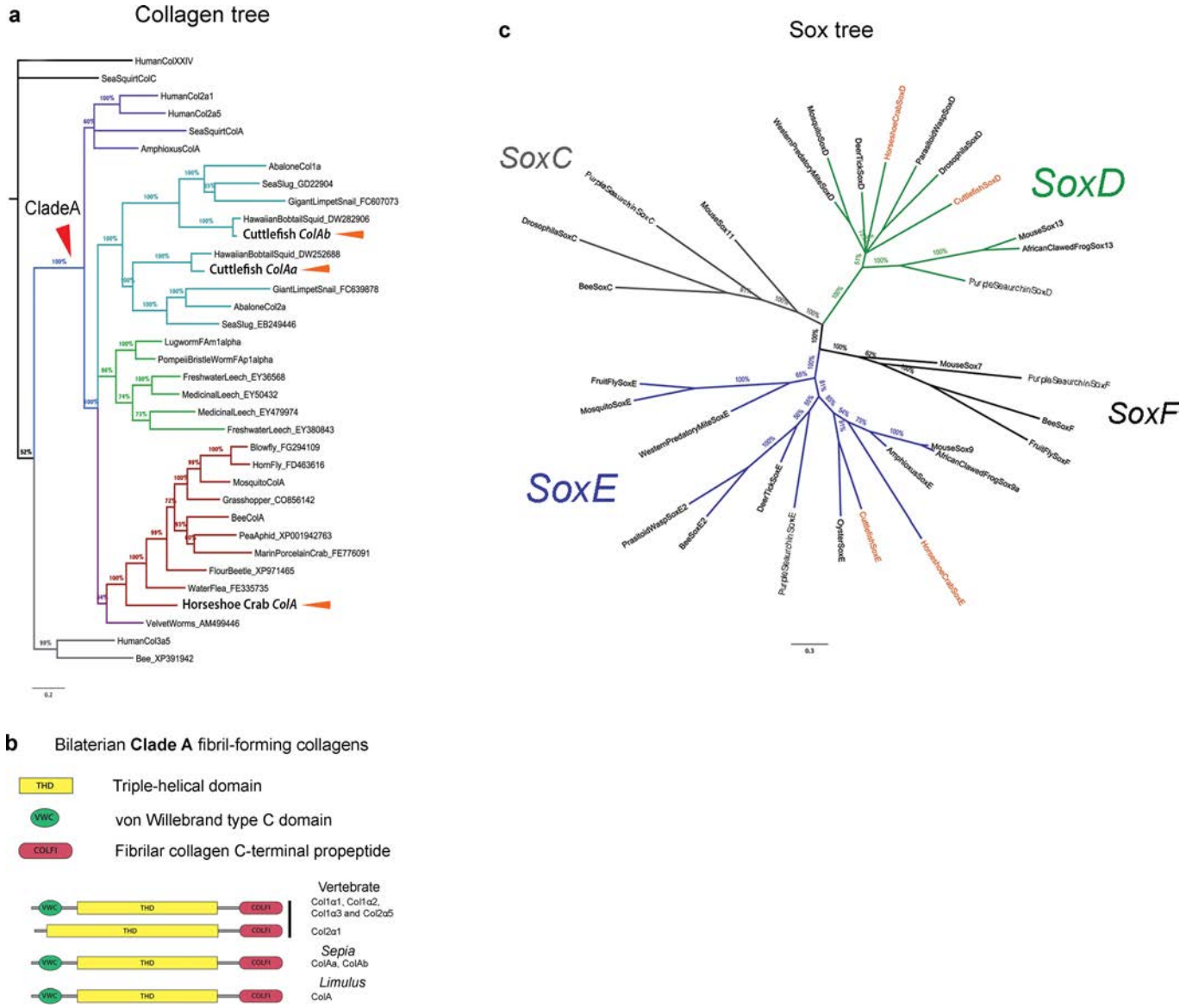

Extended Data Figure 2 | Molecular phylogenetic analysis of clade A fibrillar collagens and Sox transcription factors (*SoxC, SoxD, SoxE* and *SoxF*). a, Molecular phylogeny clade A fibrillar collagens (*ColA*) using the carboxy (C)-terminal propeptide shows that that *ColA* genes are represented in all major lineages of Bilateria (Deuterostomia, purple; Annelida, green; Mollusca, cyan; Arthropoda, red) and indicates that *Sepia* and *Limulus* (orange arrowheads) sequences belong to the *ColA* family (see Supplementary Table 1 for sequence accession numbers). **b**, Shared architecture of ColA propeptide between vertebrates and protostome invertebrates. In vertebrates, the von Willebrand type C domain is absent in Col2α1 but present in the other clade A collagens (Col1α1, Col1α2, Col1α3 and Col2α5). **c**, Molecular phylogeny of *Sox* genes using the HMG DNA binding domain under the WAG amino-acid model of evolution. The sequences derived from *Sepia* and *Limulus* (in orange) belong to the SoxE and SoxD families (see Supplementary Table 2 for sequence access numbers). All trees were generated by Bayesian phylogenetic inference using WAG model of amino-acid substitution. Branch support shown as percentage of posterior probabilities.

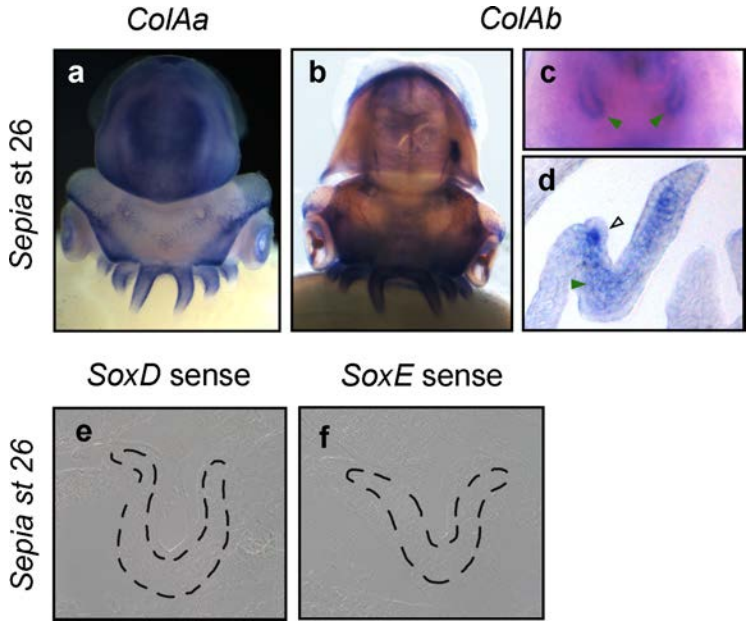

Extended Data Figure 3 | *ColAa* and *ColAb* show similar patterns of gene expression in *Sepia* embryos. a, **b**, Whole-mount ISH for (**a**) *ColAa* and (**b**) *ColAb*. Dorsal views. **c**, Ventral view of *ColAb* ISH showing the funnel cartilage precursors, marked by green arrowheads. **d**, Cryosections of these embryos reveal that *ColAb* is expressed in pre-chondrogenic mesenchyme (green arrowhead). Funnel epithelium is marked by black open arrowhead. **e**, **f**, Negative control ISH for (**e**) *SoxD* and (**d**) *SoxE* using sense RNA probes; broken lines outline pre-chondrogenic cells that form the funnel cartilage.

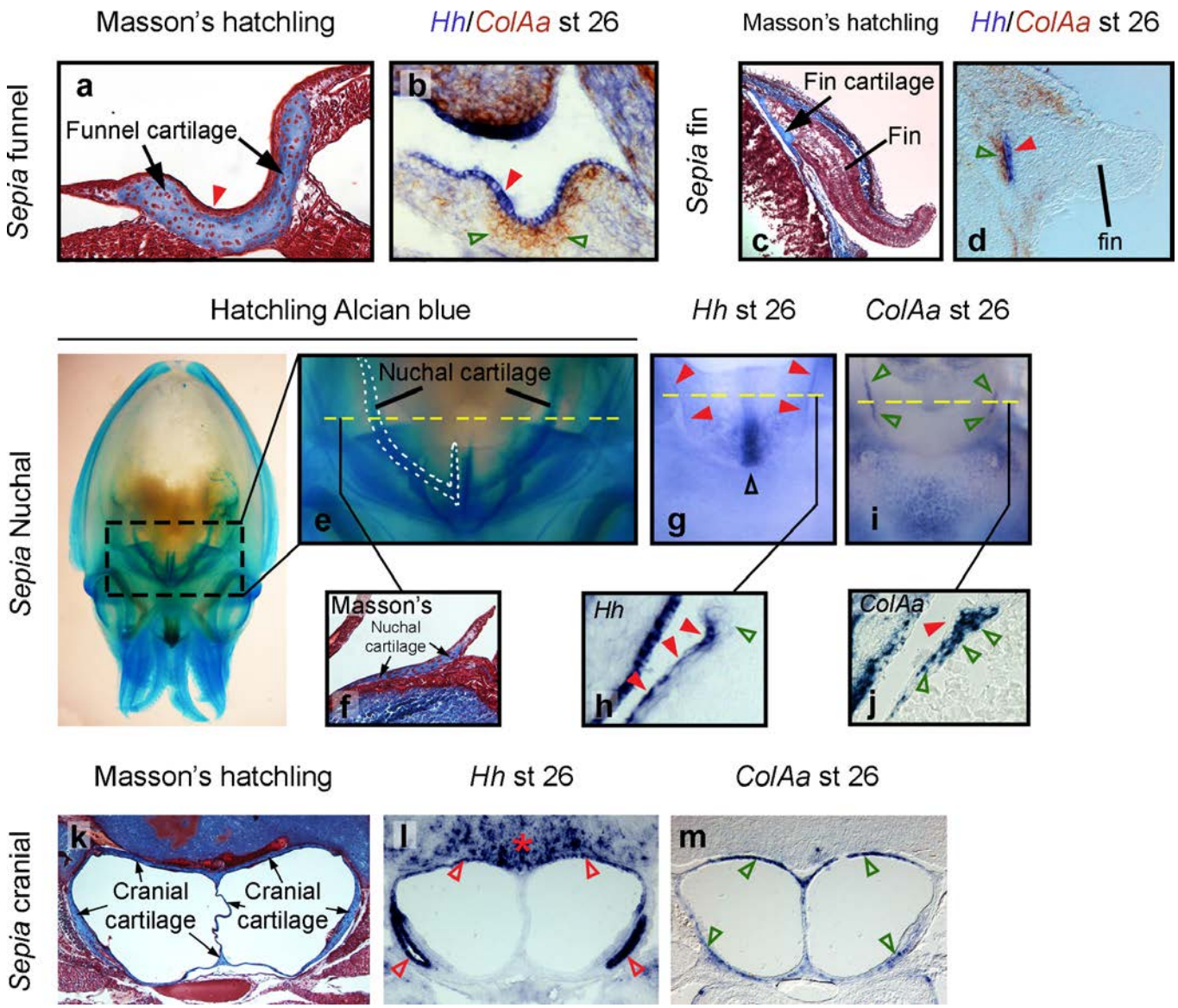

Extended Data Figure 4 | Chondrogenesis of multiple cartilages occurs near *Hedgehog*-expressing tissues in *Sepia*. **a**, Funnel cartilage in a hatchling of *Sepia* (black arrows) located underneath the funnel epithelium (red arrowhead). **b**, Double ISH of the funnel cartilage primordium at stage 26, showing the expression of *ColAa* (brown stain) in pre-cartilaginous cells (green arrowheads) and *Hedgehog (Hh*; purple stain) in the funnel epithelium (red arrowhead). **c**, Fin cartilage located at the base of the fin (black arrows) in a hatchling. **d**, Double ISH of the fin at stage 26 showing pre-cartilaginous mesenchyme expressing *ColAa* (brown stain, green arrowheads) next to a *Hh* domain (purple stain, red arrowhead). **e**, Whole-mount alcian-blue-stained *Sepia* hatchling. The white dashed outline marks the right nuchal cartilage and the yellow dashed line indicates the approximate plane of the section shown in **f**, which is stained with Masson's trichrome. **g**, Whole-mount ISH showing *Hh* expression on the right and left nuchal cartilage primordia at stage 26 (red arrowheads). A large domain of *Hh* expression can also be observed in the midline (black open arrowhead) between the nuchal cartilage primordium. Yellow dashed line in **g** indicates approximate plane of section shown in **h**, a cryosection showing the expression of *Hh* in the epithelium of the nuchal cartilage primordium (red arrowheads) but not in the mesenchyme (green open arrowhead). **i**, Whole-mount ISH of *ColAa* at stage 26 showing its expression on the nuchal cartilage primordia (green open arrowheads). Yellow dashed line in **i** indicates approximate plane of section shown in **j**, which shows a cryosection showing the expression of *ColAa* in the mesenchyme (green open arrowheads) of the nuchal cartilage primordium, but not in the epithelium (red arrowhead). **k**, Histological section stained with Masson's trichrome at the level of the paired statocyst cavities surrounded by cranial cartilages. **l**, ISH on cryosections from a stage 26 embryo reveal that the brain (marked by a red asterisk) and most of the inner epithelial lining of the statocyst cavities express *Hh* (red open arrowheads). **m**, The pre-cartilaginous cells underneath the *Hh* domain express *ColAa* (marked by green open arrowheads).

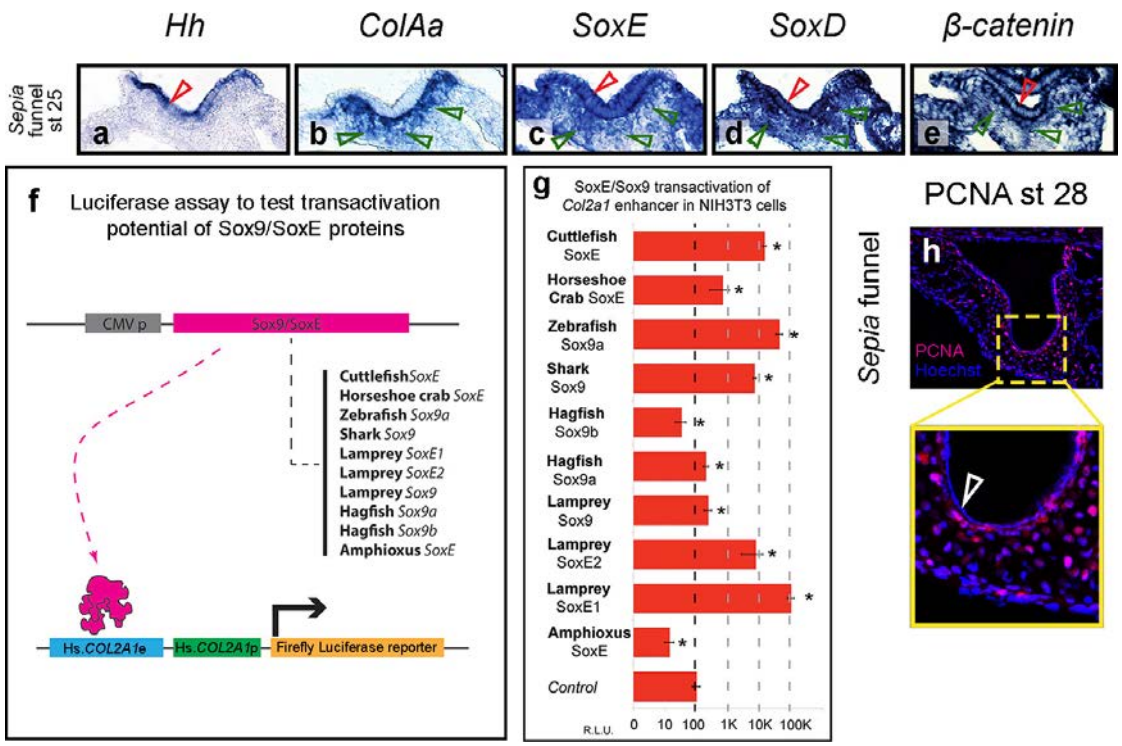

Extended Data Figure 5 | Patterns of gene expression in developing funnel cartilage of *Sepia* at stage 25. a, *Hh* is expressed in the funnel epithelium. **b**, *ColAa* is expressed in pre-cartilaginous cells. **c**, *SoxE* is expressed in the funnel epithelium as well as in the pre-cartilaginous cells, similar to **d**. **d**, **e**, *SoxD* (**d**) and *β-catenin* (**e**) expression in the funnel cartilage progenitors. In all figures, red open arrowheads mark the funnel epithelium and green open arrowheads mark pre-cartilaginous cells. **f**, Schematic representation of the luciferase reporter assay to test the transactivation potential of Sox9/SoxE transcription factors. Cells were co-transfected with a Sox9/SoxE expression vector under the control of a ubiquitous CMV promoter. The luciferase reporter was controlled by upstream *Col2a1* regulatory elements, four tandem copies of the chondrocyte-specific human *Co2a1* enhancer, and the human *Col2a1* promoter. **g**, SoxE and Sox9 transactivation of the human *Col2a1* enhancer in NIH3T3 mouse fibroblast cells, assayed by the activity of a luciferase reporter driven by the *Col2a1* enhancer. Asterisks indicate significant differences over control levels (*t*-test; $P \leq 0.05$); error bars, s.d. Each luciferase experiment was repeated four times, with four replicates per experiment. **h**, PCNA immunofluorescence in the mature funnel cartilage of stage 28 embryos indicates active proliferation in the chondrocytes over the entire cartilaginous element (bottom panel shows high magnification of boxed area above; white open arrowhead marks the epithelium). Proliferation becomes restricted to the sub-epithelial layer one stage later (compare with Fig. 3).

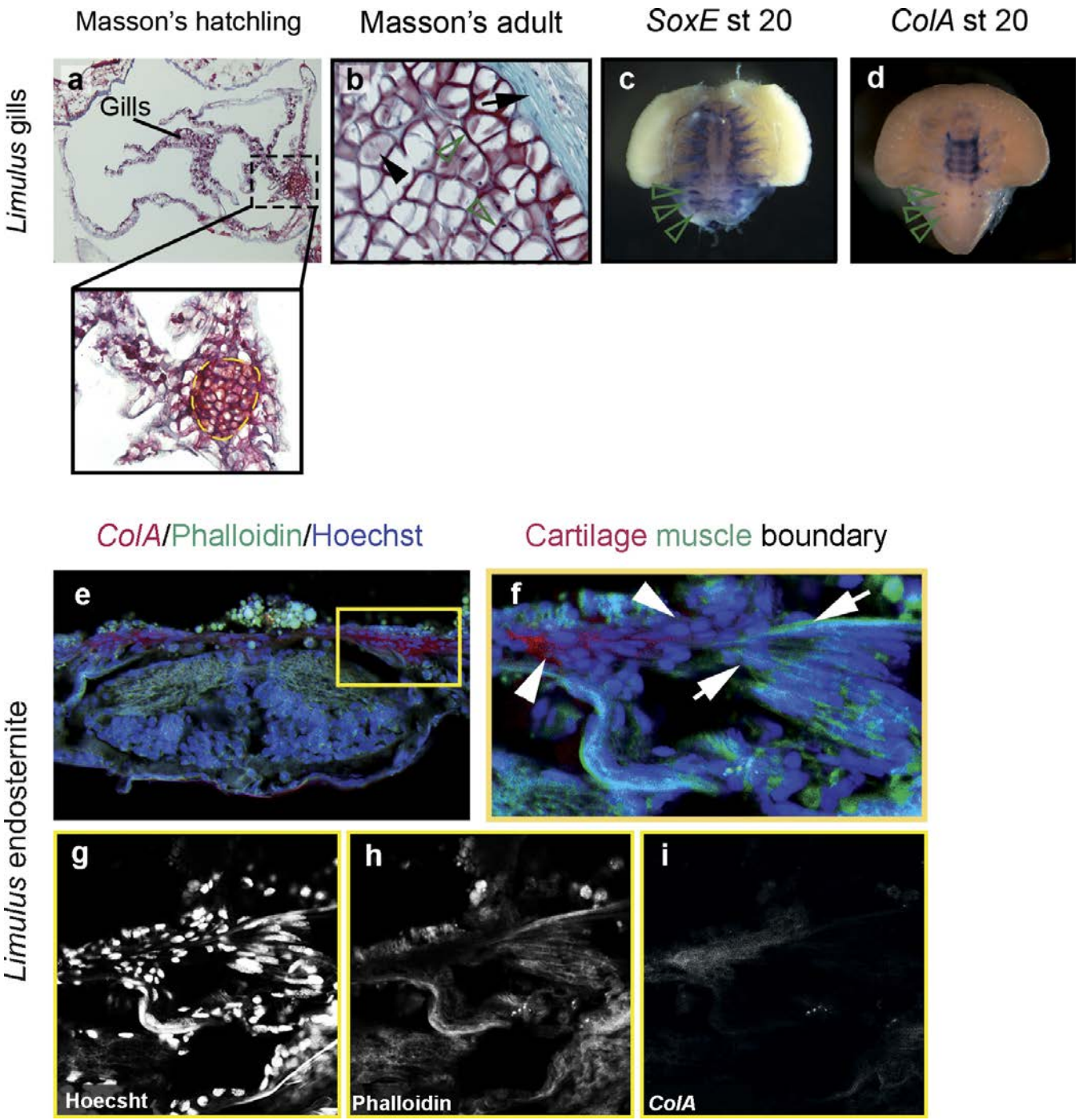

Extended Data Figure 6 | Gill and endosternite cartilages in *Limulus* are collagen-based and express *SoxE* during chondrogenesis. a, Section through gills of *Limulus* hatchlings stained with Masson's trichrome. Gill cartilage is located at the base of the gills (outlined by yellow dashed lines). **b**, Adult gill cartilage stained with Masson's trichrome showing a cell-rich tissue with hypertrophic cells (black arrowhead) separated by thin extracellular matrix (black open arrowheads); the gill cartilage ECM shows no aniline blue stain compared with the surrounding connective tissue; however, during embryonic development *SoxE* (**c**) and *ColA* (**d**) are expressed in the gill cartilage primordia (green open arrowheads). **e**–**i**, Confocal imaging of endosternite after phalloidin staining and *ColA* ISH. **f**, Higher magnification of the boxed area in **e** showing the boundary between *ColA*-expressing pre-chondrogenic cells (white arrowheads) and the differentiating muscle cells (white arrows) attached to the endosternite pre-chondrogenic tissue. **g**–**i**, Separate channels from **f**, showing Hoescht (**g**), phalloidin (**h**) and *ColA* (**i**).

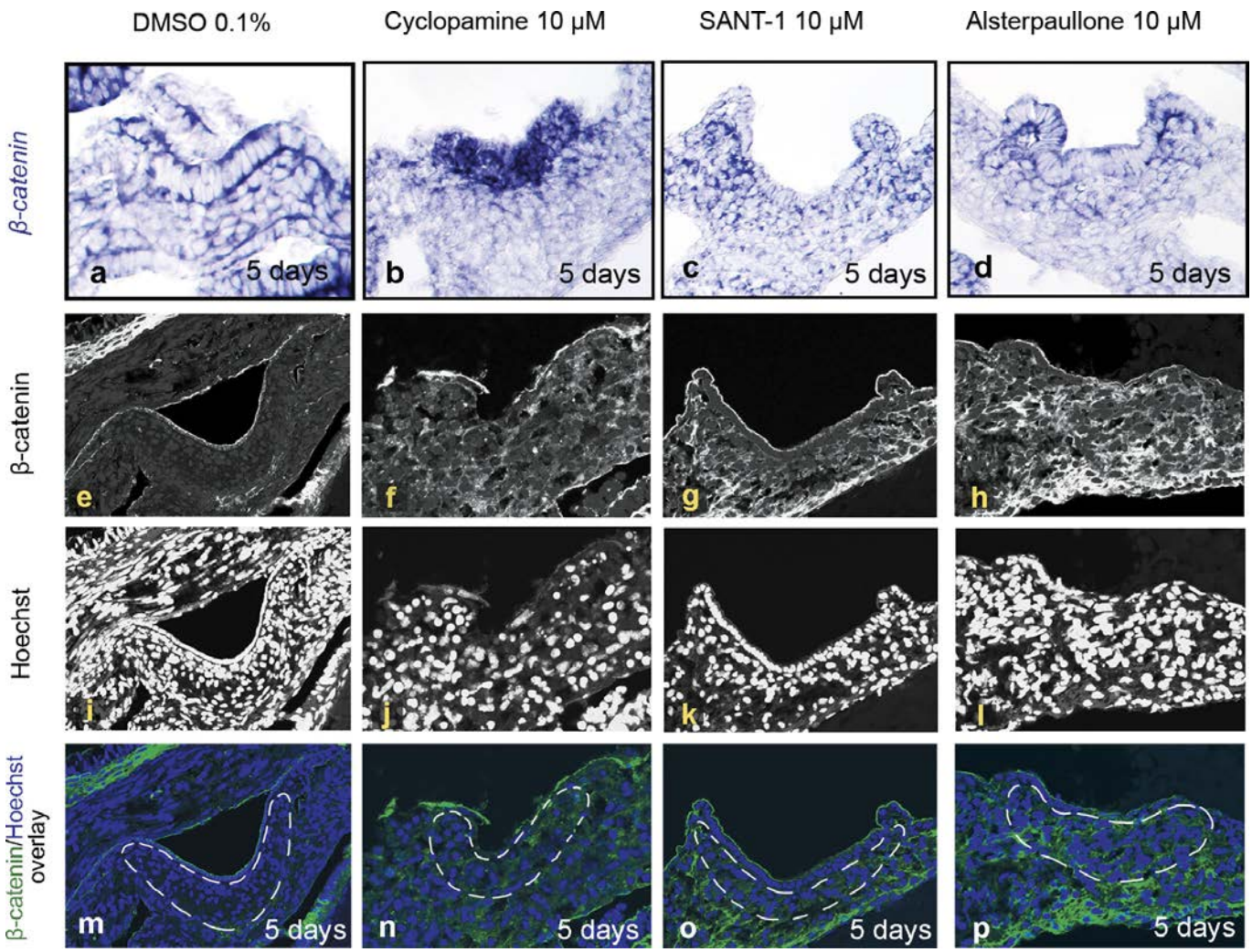

Extended Data Figure 7 | Expression of β-catenin transcripts and protein after 5-day treatments with cyclopamine, SANT-1, alsterpaullone and DMSO (control). a–d, After treatment for 5 days with small-molecule inhibitors, *β-catenin* transcripts can be detected in the funnel cartilage primordium in the (**a**) DMSO controls as well as in (**b**) cyclopamine-, (**c**) SANT-1- and (**d**) alsterpaulone-treated embryos. **e–p**, In contrast to *β-catenin* mRNA, β-catenin protein is degraded during normal funnel chondrogenesis, as seen in the DMSO control (**e**, **m**); however, β-catenin protein remains in funnel chondroprogenitors after treatment with cyclopamine (**f**, **n**), SANT-1 (**g**, **o**) and alsterpaullone (**h**, **p**).

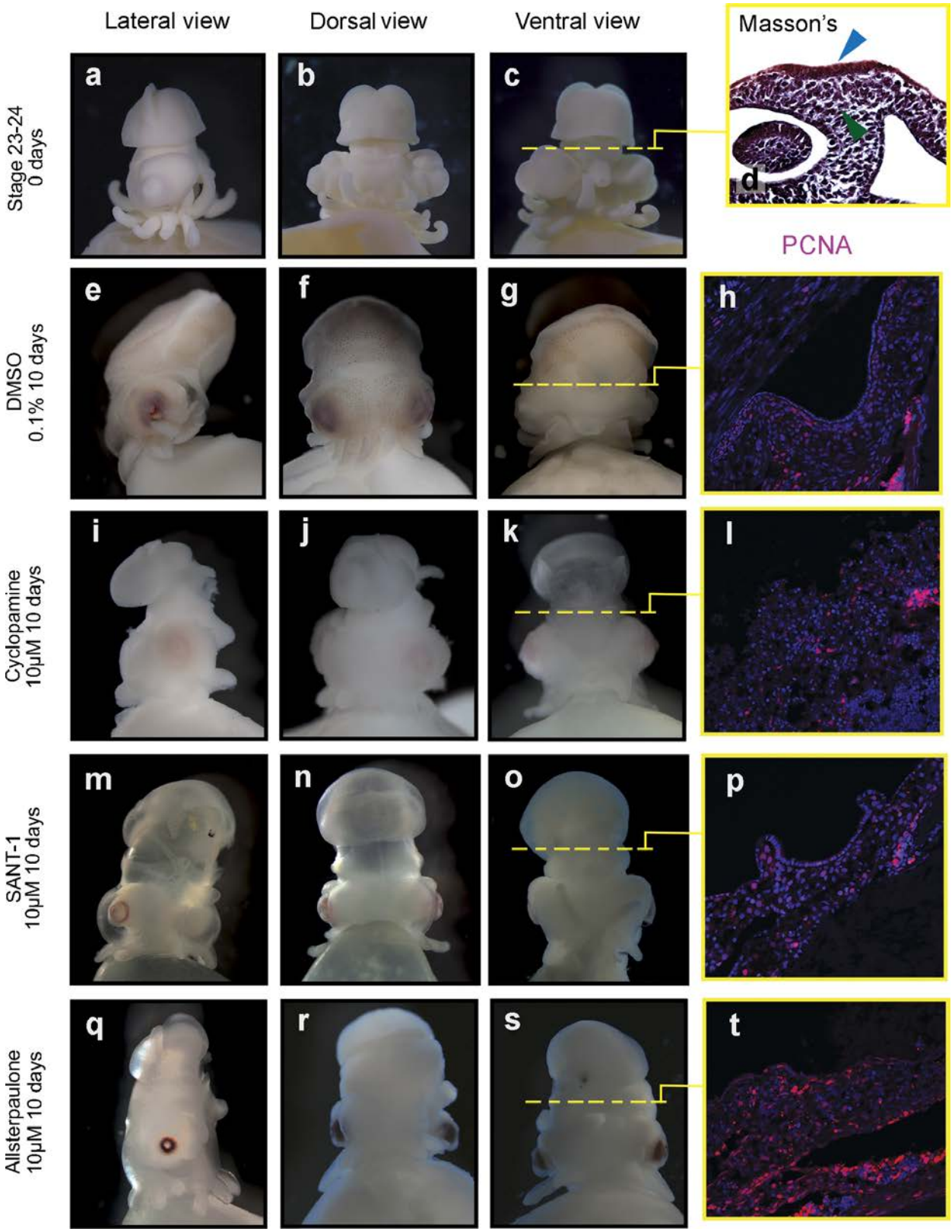

Extended Data Figure 8 | Bright-field micrographs and immunofluorescence of *Sepia* embryos before and after treatments with the small-molecule inhibitors cyclopamine, SANT-1 and alsterpaullone, or with DMSO vehicle control. a–**c**, *Sepia* embryos at the beginning of drug treatments (stages 23–24). **d**, Histological sections at the beginning of the treatments demonstrating the presence of the funnel epithelium and the associated mesenchyme. The cuboidal signalling epithelium (blue arrowhead) and pre-cartilaginous mesenchyme (green arrowhead) can be identified. **e**–**t**, *Sepia* embryos after 10 days of treatment: **e**–**g**, control DMSO-treated embryos; **i**–**k**, cyclopamine-treated embryos; **m**–**o**, SANT-1-treated embryos; **q**–**s**, alsterpaullone-treated embryos. **h**, **l**, **p**, **t**, PCNA staining shows that cell proliferation in funnel cartilage continued after drug treatments, indicating that treatments did not induce global toxicity. DMSO control (**h**) cyclopamine- (**l**) and SANT-1-treated (**p**) embryos stained positive for cell proliferation in the funnel cartilage, and alsterpaullone-treated (**t**) embryos showed stronger PCNA staining of the funnel cartilage than did cyclopamine-treated embryos, SANT-1-treated embryos or DMSO controls.

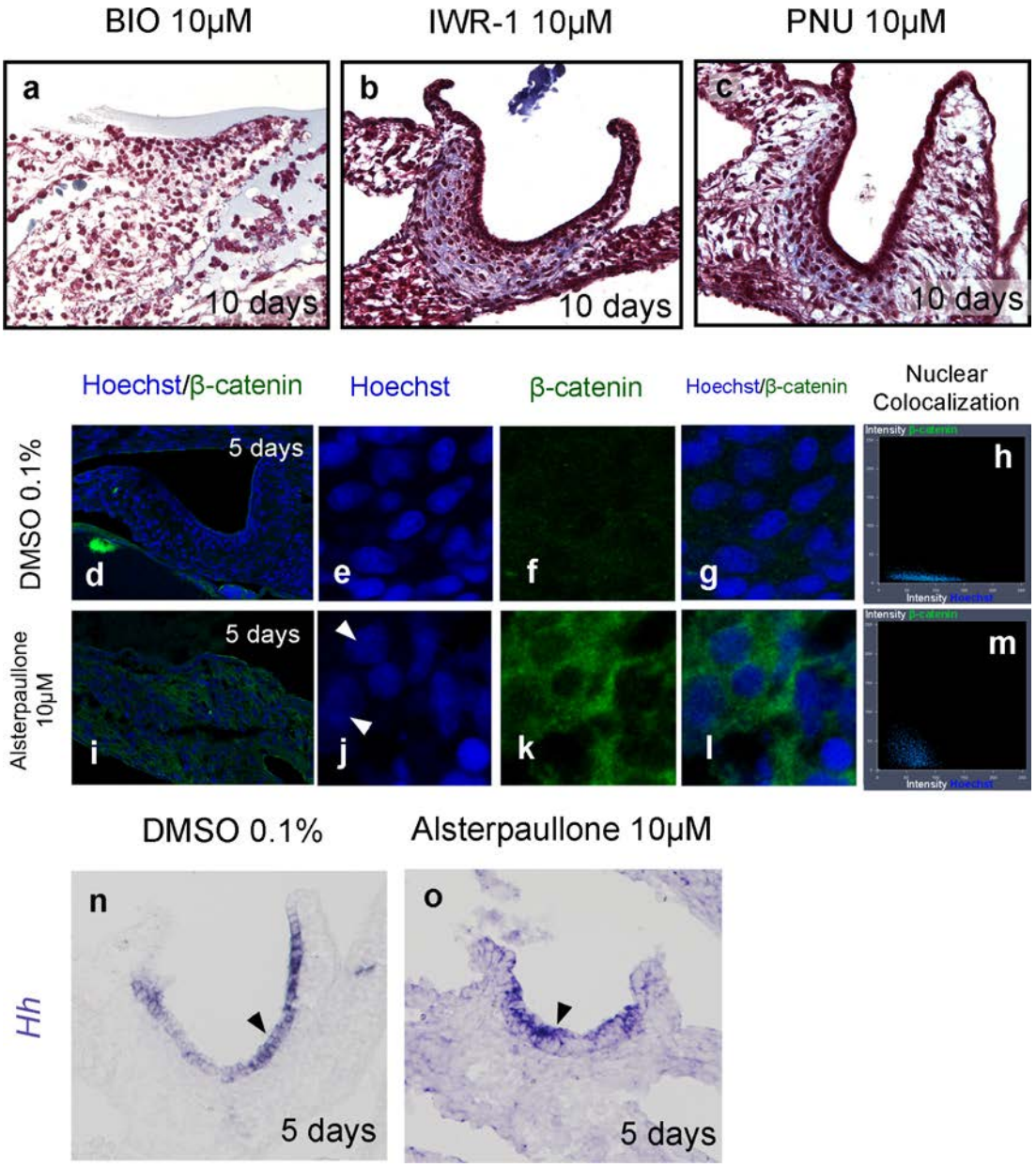

Extended Data Figure 9 | Positive and negative modulation of β-catenin signalling has opposite effects on chondrogenesis in *Sepia*. **a**, Stabilization of β-catenin signalling using the GSK-3β inhibitor BIO prevents funnel cartilage development, as revealed by Masson's trichrome. **b**, **c**, Inhibition of β-catenin signalling by inducing axin stabilization (stabilization of β-catenin destruction complex) with IWR-1 (**b**) or by blocking the interaction of β-catenin and Tcf with PNU (**c**), did not disrupt chondrogenesis of funnel cartilage. **d**–**g**, **i**–**l**, Cellular accumulation of β-catenin in funnel cartilage of alsterpaullone-treated embryos compared with DMSO controls. β-catenin nuclear localization is not observed in DMSO control embryos (**d**–**g**), but after alsterpaullone treatment, β-catenin accumulates in the cytoplasm and the nucleus (**i**–**l**). Arrowheads mark two cells stained with Hoechst (**j**) that are rich in β-catenin (**k**). **g**, **l**, Overlay of Hoechst/β-catenin from **e** and **f** (**g**) and **j** and **k** (**l**). **h**, **m**, Nuclear co-localization plots of funnel cartilage cells showing β-catenin intensities in Hoechst-positive domains (nuclei); cytoplasmic β-catenin signal is not plotted. Alsterpaullone-treated embryos (**m**) show higher β-catenin intensities than DMSO controls (**h**), demonstrating β-catenin accumulation in the nuclei. **n**–**o**, Accumulation of β-catenin does not affect Hh expression in the funnel epithelium after alsterpaullone treatments; compare **o** with DMSO controls in **n**.